Surface relaxation in liquid water and methanol studied by x-ray absorption spectroscopy

Kevin R. Wilson, R. D. Schaller, D. T. Co, and R. J. Saykally[a)]
Department of Chemistry, University of California, Berkeley, California 94720

Bruce S. Rude, T. Catalano, and J. D. Bozek
Advanced Light Source, Lawrence Berkeley National Laboratory, Berkeley, California 94720

(Received 17 May 2002; accepted 30 July 2002)

X-ray absorption spectroscopy is a powerful probe of local electronic structure in disordered media. By employing extended x-ray absorption fine structure spectroscopy of liquid microjets, the intermolecular O–O distance has been observed to undergo a 5.9% *expansion* at the liquid water interface, in contrast to liquid methanol for which there is a 4.6% surface *contraction*. Despite the similar properties of liquid water and methanol (e.g., abnormal heats of vaporization, boiling points, dipole moments, etc.), this result implies dramatic differences in the surface hydrogen bond structure, which is evidenced by the difference in surface tension of these liquids. This result is consistent with surface vibrational spectroscopy, which indicates both stronger hydrogen bonding and polar ordering at the methanol surface as a consequence of ''hydrophobic packing'' of the methyl group. © *2002 American Institute of Physics.* [DOI: 10.1063/1.1508364]

INTRODUCTION

The surfaces of metals, alloys, semiconductors, and insulators all exhibit structural relaxation relative to the underlying bulk material. Electron diffraction of clean metal surfaces in vacuum has shown that the spacing between the first and second atomic layers of these systems often exhibits a contraction relative to the bulk geometry and, occasionally, an outward expansion in the first few atomic layers.[1] In extreme cases, solid surfaces actually reconstruct, adopting a different atomic arrangement than the underlying bulk crystal structure. These effects are driven by the anisotropic force at the interface that results from the reduction of coordination number and bond order in the surface layer. One might expect similar behavior to occur in molecular liquids, engendering the familiar properties of surface tension, but quantitative experimental measurements of liquid surface structure have been technically prohibitive. Here we report the surface relaxation of the near-neighbor O–O distance in methanol and water, exploiting the surface sensitivity of ion-yield extended x-ray absorption fine structure (EXAFS) of liquid microjets.

Model radial distribution functions (RDF) have been extracted from the analysis of neutron and x-ray diffraction data for both liquid methanol and water.[2–5] The atom pair correlation function enumerates the short-range order, yielding average radial distances and coordination numbers. Ambient (25 °C) water exhibits a broad maximum in the RDF at ~2.85 Å with an average coordination number of 3.6; however, some debate still remains regarding the exact location and shape of this first maximum in the RDF, as discussed by Hura *et al.*[6] Liquid methanol exhibits a similar O–O feature at an intermolecular distance of 2.76 Å, which is shorter than that of liquid water, with an average coordination number of ~2.[7] Despite this shorter intermolecular O–O distance, liquid methanol is 25% less dense than water, indicating significant differences in hydrogen bond morphology relative to the three-dimensional hydrogen bond network present in bulk liquid water. Until now, analogous structural information could not be readily obtained for the surfaces of these liquids.

The surface tension of liquid water is large (75 erg/cm^2) relative to that of methanol (22 erg/cm^2). This latter value is typical of pure hydrocarbon interfaces, implying that instead of the —OH termination of the liquid surface found for water, methanol molecules are polar oriented with the methyl group extending out of the liquid surface. Sum frequency generation (SFG) spectroscopy, in which the surface vibrational spectrum can be obtained, provided the first detailed insights into the molecular ordering of these liquid/vapor interfaces. The water surface exhibits a narrow OH vibrational resonance at 3685 cm^{-1}, assigned to a single hydrogen bond donor with an average dipole moment parallel to the surface, implying that the broken hydrogen bond extends out of the surface by ca. 38°.[8] Furthermore, by surface titration, Du *et al.*[8] determined that molecules possessing such a dangling OH bond accounted for ~25% of the surface.

SFG studies by Stanners *et al.*[9] and Wolfrum *et al.*[10] of liquid methanol surfaces revealed that the methyl group extends out of the bulk, with a broad orientational distribution about the surface normal. Similar results have been obtained for ethanol, longer chain alcohols, and surfactants in which the larger alkyl group enhances this hydrophobic effect.

Molecular dynamics (MD) computer simulations of liquid/vapor interfaces yield molecular-level information not readily available in modern experiments. A number of such simulations, employing a variety of intermolecular potential functions, have been reported for the equilibrium liquid water interface.[11–15] Generally, the liquid/vapor water interface

a)Author to whom correspondence should be addressed. Electronic mail: saykally@uclink4.berkeley.edu

was determined to be 1–1.5 molecular diameters or ~5 Å thick, with the average number of hydrogen bonds per interfacial molecule determined to be ~2, reduced from the bulk value of ~4.[12] Single donor hydrogen bonded species, consistent with the ''free OH'' oscillator, have indeed been observed. Dang and Chang[13] found that the average dipole moments of molecules in this interfacial region rapidly relax toward gas phase values. Alejandre *et al.*[15] showed that with appropriate long-range corrections (dipole–dipole interaction) to the SPC/E potential, the computed surface tension was in good agreement with experimental values.

Simulations of the methanol surface, conducted by Matsumoto and Kataoka,[16] yield many interfacial properties similar to those reported for water. Using the transferable intermolecular potential function (TIPS), the methyl groups were observed to extend out of the liquid surface, in accordance with SFG results. Surprisingly, the thickness of the methanol interface was observed to be ~8 Å, nearly twice that of water. However, it is unclear whether this interfacial expansion is an artifact of the simplistic TIPS potential.

The availability of reliable intermolecular distances for interfacial regions of hydrogen bonding liquids could significantly enhance our understanding of the molecular details of surface phenomena, which include evaporation, condensation, and surface free energy. In addition, such structural information provides new benchmarks for developing realistic liquid models. However, there are few experimental techniques that can be employed in the analysis of liquid surface structure. Most ''traditional'' surface science techniques—e.g., low-energy electron diffraction (LEED)—are complicated by the large equilibrium vapor pressure above most molecular liquids which obscures direct interrogation of the liquid surface. X-ray absorption techniques combined with liquid microjet targets provide a novel method for examining the electronic and geometric structure of liquid surfaces.[17,18] In particular, EXAFS, a standard tool for the investigation of the local electronic structure of disordered materials such as liquids, glasses, and amorphous solids, can now be applied to study volatile liquid surfaces.

EXAFS refers to the small-amplitude oscillations in the x-ray absorption coefficient that can extend hundreds of electron volts above a core-level absorption edge. These oscillations arise from final-state interference effects of backscattered photoelectrons from neighboring atoms. The well-known utility of EXAFS as a structural probe arises largely from the ability to selectively excite individual atomic species, thereby allowing the local environment (e.g., solvent cage) around a selected atom to be directly probed. Within the single-scattering formalism,[19] modulation in the absorption coefficient ($\Delta\mu$) for *K*-edge spectra normalized to the isolated atomic background (μ_0) is given by

$$\chi(k)=\frac{\Delta\mu}{\mu_0}=-\sum_j \frac{S(k)N_j}{kr_j^2}|f_j(k,\pi)| \times \sin[2kr_j+\varphi_j(k)]e^{-2\sigma_j^2k^2}, \qquad k=\sqrt{\frac{2m}{\hbar^2}(E-E_0)}, \tag{1}$$

where N_j is the number of nearest neighbors, k the photoelectron wave vector, and $f_j(k,\pi)$ the scattering amplitude. $S(k)$ is an amplitude reduction term due to many-body effects, and r_j is the radial distance from the absorbing atom. Mean-square fluctuations in r_j are accounted for in the exponential Debye–Waller factor (σ_j), and $\varphi_j(k)$ accounts for the total phase of the curved-wave scattering amplitude along the scattering trajectory. Analysis of the EXAFS function $\chi(k)$ yields atom pair correlations functions, thus allowing accurate determination of near-neighbor distances and coordination numbers.

The EXAFS absorption coefficient can be probed directly, as in traditional transmission experiments, or indirectly by detecting the emission of secondary electrons, ions, neutrals, or fluorescent photons produced by Auger decay. Furthermore, each of these emitted particles have characteristic escape depths.[20] For example, fluorescent photons that are nonresonant with any sample component will have an escape depth of many micrometers, while secondary electrons, which dominate the total electron yield (TEY), escape from an average depth of 20 Å, determined by the average kinetic energy distribution. Ions, atoms, or molecules desorb directly from the interface, sensitive to only the outermost surface layer (1–5 Å).[20] By separately measuring the total ion yield (TIY) and TEY as a function of x-ray excitation energy, EXAFS spectra of the liquid surface and bulk can be simultaneously obtained. We have observed no differences between the near-edge x-ray absorption fine structure spectra (NEXAFS) measured by TEY and fluorescence yields, indicating that bulk electronic properties are probed in both cases.[18]

EXPERIMENT

To investigate water and simple alcohols, EXAFS spectra were recorded at the oxygen *K* edge (530 eV) requiring a synchrotron light source and an endstation that can couple volatile liquids into ultrahigh vacuum. These experiments were conducted at the Advanced Light Source, beamline 8.0 Lawrence Berkeley National Laboratory. This undulator beamline produces 10^{12} photon/sec at 500 eV, delivering a 80×80 μm^2 spot size, suitable for the interrogation of a 20-μm-diam liquid target without appreciable interference from the surrounding gas phase. The experiment has been described elsewhere.[17] The liquid microjet endstation consists of three stages of differential pumping and an interaction chamber. A 20-μm-diam liquid jet of H_2O or methanol is injected into the interaction region in which the x-ray beam intersects the liquid jet at 90°. After traveling 5 mm, the liquid jet is directed through a 300-μm-diameter skimmer and dumped 1 m away on a liquid nitrogen trap. The interaction region is maintained at 1×10^{-5} torr for liquid water and 4×10^{-5} for methanol by a 1000-l/sec turbopump located behind a liquid nitrogen trap. The final stage of the differential pumping section is maintained at 1×10^{-9} torr during normal operation. The TIY-TEY EXAFS spectra were recorded with an instrumental resolution of 1.0 eV. Figure 1 shows a typical EXAFS spectrum obtained for a 20-μm liquid methanol jet at the carbon (280 eV) and oxygen *K* edges (530 eV).

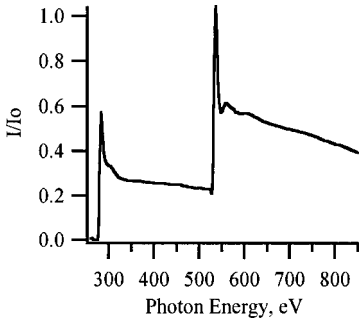

FIG. 1. Carbon and oxygen *K*-edge x-ray absorption spectrum of liquid methanol measured by TEY (I) normalized to the incoming photon intensity (I_0).

RESULTS AND ANALYSIS

To obtain quantitative near-neighbor distances and coordination numbers, reliable phase, $\varphi_j(k)$, and amplitude $f(k)$, functions must be used.[21] These functions can be computed directly from multiple-scattering codes (e.g., FEFF 8.0 or GNAXS) or extracted experimentally from model systems in which coordination numbers and distances have been previously determined. The latter procedure was used by our group to determine the OH phase shift function for molecular water.[22] Yang and Kirz[23] demonstrated in the first EXAFS study of liquid water that the O–O distance was underdetermined by 10% when a phase shift function computed by Teo and Lee[24] was used. The presence of hydrogen atoms in nearly collinear paths with neighboring water molecules can lead to focusing effects and additional phase shifts that must be accounted for in any O–O phase shift function used in the analysis of hydrogen bonding liquids. Bowron *et al.*,[25] in a recent x-ray Raman EXAFS study of liquid water, accounted for such effects and obtained an intermolecular O–O distance of 2.87 Å, consistent with previous neutron and x-ray diffraction studies. We have extracted their O–O phase shift function, shown in Fig. 2, and use it consistently in all of the O *K*-edge EXAFS analysis of both liquid water and methanol. For consistency, $\chi(k)$ was extracted using $E_0 = 538.9\,\mathrm{eV}$ for all spectra reported here. In the same way, accurate determination of coordination number requires a suitable amplitude function to adequately constrain the subset of highly correlated variables such as coordination number and Debye–Waller factor. The amplitude function $f(k)$, shown in Fig. 2, was also extracted from the data of Bowron *et al.*[25] and used throughout this analysis.

The raw k^3-weighted EXAFS spectra $k^3\chi(k)$ for liquid water recorded by TEY and TIY are shown in Figs. 3 and 4, respectively. Also shown is the Fourier-filtered oscillation revealing the presence of a single dominant near-neighbor distance. The raw data were first Fourier transformed with a Kaiser–Bessel window function ($3 \geqslant k \geqslant 8\,\mathrm{Å}^{-1}$), filtered, and then backtransformed using a Gaussian window for fitting in k space. One can clearly discern a qualitative difference in the phase of the oscillation measured for the surface and bulk. Also included are model fits in k space to the backtransformed oscillation obtained with a standard EXAFS analysis package.[26] The results of the respective fits are given in Table I accompanied by an error analysis as

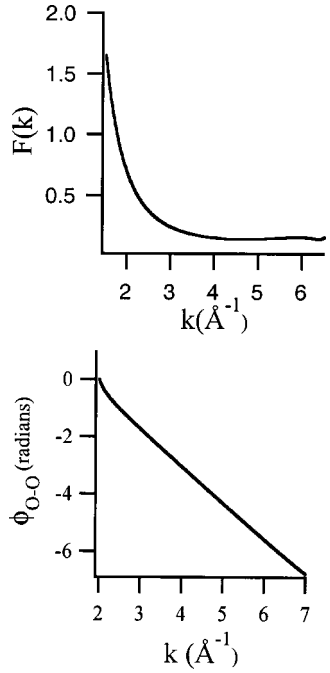

FIG. 2. Amplitude function $f(k)$ (top) and O-O phase shift function $\varphi(k)$ (bottom).

described in Ref. 26. The respective fits were conducted in k space on the backtransformed oscillations, yielding relatively small k^3-weighted residuals, as shown in Figs. 3 and 4 and Table I. To explicitly account for experimental errors, each parameter was adjusted to estimate the associated standard deviation and they are also reported in Table I. The residuals include experimental noise as well as weak oscillations originating from the second-coordination shell. Unfortunately, the signal-to-noise ratio did not permit accurate quantification of these long-range correlations.

Before the intermolecular O–O distance in liquid methanol could be extracted, oscillations due to the intramolecular C–O distance must be removed. This was done by measuring the EXAFS spectra for methanol vapor and extracting

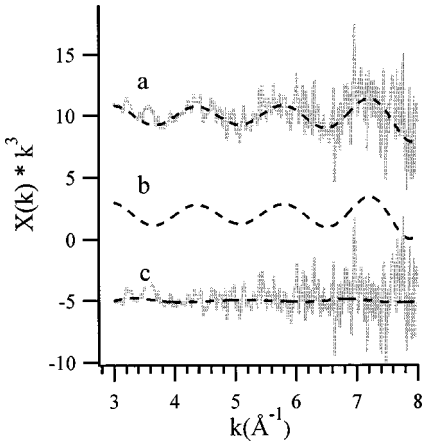

FIG. 3. k^3-weighted liquid water microjet oxygen *K*-edge TEY EXAFS spectrum $\chi(k)$. (a) Raw data (solid line) and back Fourier transformed (BFT) oscillation (dashed line). (b) Model fit to the backtransformed data. (c) Fit residuals from the raw (solid line) and BFT (dashed line) $\chi(k)$.

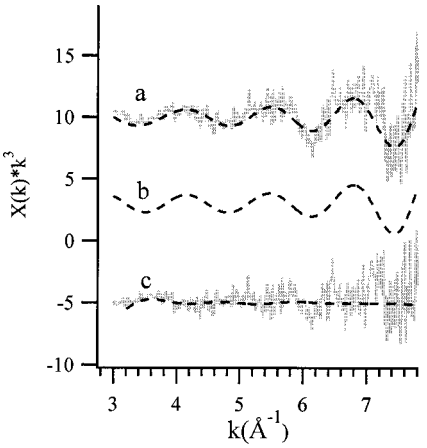

FIG. 4. k^3-weighted liquid water microjet oxygen *K*-edge TIY EXAFS spectrum $\chi(k)$. (a) Raw data (solid line) and back Fourier transformed (BFT) oscillation (dashed line). (b) Model fit to the backtransformed data. (c) Fit residuals from the raw (solid line) and BFT (dashed line) $\chi(k)$.

$\chi(k)$ as shown in Fig. 5. The low-frequency intramolecular oscillation was removed from the liquid data either by Fourier filtering or with a direct subtraction procedure, both yielding equivalent results. This is analogous to fitting an atomic background function to retrieve molecular distances as done for H_2O in Ref. 22. The subtraction procedure is more reliable when the intra- and intermolecular distances are well separated in *R* space as is the case for methanol. Liquid ethanol EXAFS spectra were also measured, but the intramolecular C–C–O distance overlapped with the intermolecular O–O distance, making it more difficult to extract a background-independent $\chi(k)$. After removing the intramolecular component, the same analysis that was applied to liquid water was conducted on the k^3-weighted O *K*-edge EXAFS spectra of liquid methanol, recorded by TEY and TIY. The results are shown in Figs. 6 and 7, respectively. The same fitting procedure and error analysis as described above were employed, the results of which are given in Table II.

Analysis of the TEY EXAFS spectra yields O–O distances consistent with previous diffraction studies of both bulk liquid water and methanol. Bulk liquid water (TEY) was found to yield $R_{O-O}=2.80\pm0.05$ Å, which is slightly shorter than the first maximum in the radial distribution function determined by some neutron and x-ray diffraction studies. Recently, a new set of x-ray scattering data[6] extracted a model RDF implying a more structured liquid, evidenced by a taller and sharper first $G(r)_{O-O}$ and a significantly shorter first maximum, $R_{O-O}=2.73$ Å. For comparison, hexagonal

TABLE I. Intermolecular parameters [Eq. (1)] and errors determined in the single-scattering EXAFS analysis of liquid water. The surface O–O distance (R_{O-O}) exhibits a 5.9% expansion relative to the bulk liquid.

Parameter	TEY fit (back FFT/exp error)	TIY fit (back FFT/exp error)
R_{O-O} (Å)	2.801(±0.019/0.05)	2.965(±0.029/0.05)
N	1.38(0.41/2)	1.07(0.3/1.5)
σ (Å^{-2})	0.009 58(0.002/0.006)	0.001 93(0.002/0.004)
ΔE_0	4.634(2.98/3.05)	6.824(3.713/4.81)
$S(k)$	0.80	0.80

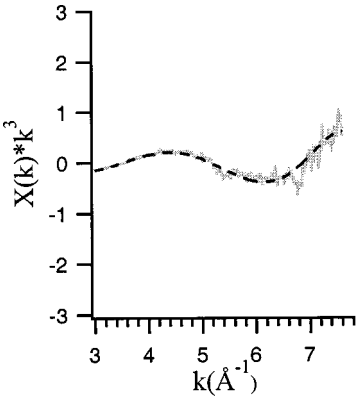

FIG. 5. k^3-weighted oxygen *K*-edge TEY EXAFS spectrum recorded for methanol vapor.

ice is tetrahedrally coordinated with an O–O distance of 2.76 Å. Analysis of the TEY methanol spectrum yielded $R_{O-O}=2.75\pm0.05$ Å, which is shorter than bulk water and in good agreement with previous diffraction studies ($R_{O-O}=2.72$ Å).[27]

Analysis of the surface sensitive TIY spectra yielded a $R_{O-O}=2.96\pm0.05$ Å for liquid water. This represents a 5.9% *expansion* of the near-neighbor distance at the water surface when compared with the results obtained from the bulk TEY spectrum. In a previous study we reported the same 5% elongation of the near-neighbor distance with slightly different absolute values for the bulk and surface R_{O-O}.[17] This merely reflects slight differences in the O–O phase function used in that study. Here we used the O–O phase shift function derived from Bowron *et al.*,[25] which is more reliable since it was directly determined from hexagonal ice which is an extensively characterized model system. The surface R_{O-O} for liquid methanol is determined here to be 2.62 ± 0.05 Å, yielding a 4.6% *contraction* of the intermolecular O–O distance relative to the bulk liquid.

In order to constrain the number of parameters used in the determination of coordination number and Debye–Waller factor, $S(k)$, the amplitude reduction term due to multiple excitations, was fixed at a value of 0.8, which is consistent with a previous EXAFS study of water.[22] For the liquid wa-

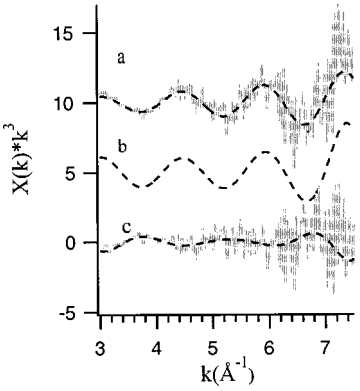

FIG. 6. k^3-weighted liquid methanol microjet oxygen *K*-edge TEY EXAFS spectrum $\chi(k)$. (a) Raw data (solid line) and back Fourier transformed (BFT) oscillation (dashed line). (b) Model fit to the backtransformed data. (c) Fit residuals from the raw (solid line) and BFT (dashed line) $\chi(k)$.

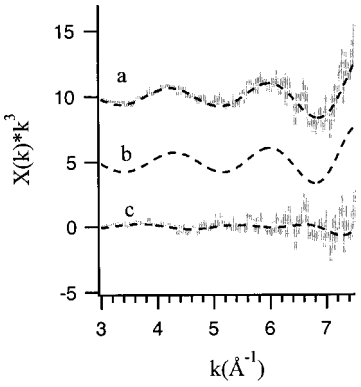

FIG. 7. k^3-weighted liquid methanol microjet oxygen *K*-edge TIY EXAFS spectrum $\chi(k)$. (a) Raw data (solid line) and back Fourier transformed (BFT) oscillation (dashed line). (b) Model fit to the backtransformed data. (c) Fit residuals from the raw (solid line) and BFT (dashed line) $\chi(k)$.

ter surface, N_j was observed to decrease by 22% relative to the bulk, while the coordination number at the surface of liquid methanol shows a 41% reduction. While the relative reduction in coordination numbers at the surface of methanol and water are in fair agreement with MD simulations,[12,16] the coordination numbers themselves appear to be unrealistically small and are accompanied by large fitting errors. This may result from inaccuracies in the amplitude function $f(k)$. Furthermore, Filipponi[28] has pointed out that realistic model RDF's that exhibit the correct long-range behavior $[\lim_{r\to\infty} g(r)=1]$ and compressibility limit should be considered in the analysis of disordered media. The single-shell approximation, used in the present analysis, has been shown to underdetermine coordination numbers as well as Debye–Waller factors.[29] Performing such an analysis on liquid surfaces is complicated by the inherent nature of the interface, in which the density drops by orders of magnitude over several molecular diameters. In addition, it is unclear what would constitute the correct compressibility limit for these interfacial systems. More theoretical work is clearly needed to investigate the applicability of such a scheme to the analysis of liquid surface EXAFS spectra.

DISCUSSION

Despite the apparent similarity of bulk methanol and water, the expansion of the O–O distance observed at the liquid water surface and the corresponding contraction in liquid methanol clearly indicate significant differences in the interfacial hydrogen bond network. This result is underscored by the difference in surface tension measured for these liquids.

TABLE II. Intermolecular parameters [Eq. (1)] and errors determined in the single-scattering EXAFS analysis of liquid methanol. The surface O–O distance exhibits a 4.6% contraction relative to the bulk liquid.

Parameter	TEY fit (back FFT/exp error)	TIY fit (back FFT/exp error)
R_{O-O} (Å)	2.755(±0.03/0.05)	2.628(±0.042/0.07)
N	1.34(0.6/3.0)	0.788(0.9/1.5)
σ (Å^{-2})	0.0020(0.002/0.008)	0.0032(0.005/0.009)
ΔE_0	4.578(3.02/4.03)	−9.795(4.98/7.87)
$S(k)$	0.80	0.80

In methanol, the presence of the methyl group is known to disrupt the three-dimensional tetrahedral hydrogen bond network comprising liquid water, instead forming parallel winding chains, as in solid methanol, or planar cyclic clusters.[27] These differences in hydrogen bond topology might be expected to have large effects on the local structure of these interfaces. MD simulations show that while interfacial water molecules are weakly oriented, the methanol surface exhibits stronger orientation of molecular dipoles and is stabilized by expelling the hydrophobic methyl group out of the surface.[16] This picture is supported by the absence of a ''free OH'' resonance in the surface SFG spectra of liquid methanol.[9]

The expansion of the O–O distance at the liquid water surface, along with our recent NEXAFS study which identified a new group of hydrogen-bond ''acceptor-only'' surface species,[18] implies a significant relaxation of the electronic perturbation due to intermolecular hydrogen bonds at the liquid/vapor interface. This can be rationalized by an overall reduction in the number of surface hydrogen bonds per water molecule, as predicted by MD simulations, as well as lengthening of the near-neighbor distance, which would weaken the remaining hydrogen bonds between surface molecules. This view implies an interfacial layer in which water molecules exhibit enhanced mobility, as evidenced by an interfacial diffusion constant computed to be ~54% larger than the bulk value.[11]

Although there is no direct experimental evidence for dimerization at the liquid/vapor interface of water, the R_{O-O} reported here is similar to that observed in the isolated water dimer. Far-infrared cluster studies have shown that the O–O distance decreases with increasing water cluster size.[30] The intermolecular O–O distance is observed to be 2.952 Å for the dimer, converging to a value of 2.75 Å for the water pentamer, in which nearly linear hydrogen bonds form tetrahedral bonding geometry. This trend illustrates the importance of cooperative effects on the hydrogen bond length and, consequently, on the near-neighbor O–O distance.

It is well known in a variety of hydrogen bonding systems that the covalent OH distance is sensitive to the hydrogen bond strength, which is itself a function of bond length and angle. Strong intermolecular hydrogen bonds redistribute electron density which weakens the intramolecular OH bond, resulting in covalent bonds that are 1%–2% longer in the liquid than in isolated water monomers. Experimentally, the OH stretching frequency is observed to ''redshift'' with increasing number of hydrogen bonds and bond strength—indicating a weakening of the covalent OH force constant upon formation of a hydrogen bond.[31] Townsend and Rice[11] observed a 0.4%–0.7% contraction of the covalent OH distance and a 1%–2% increase in the HOH angle as molecules moved from the bulk toward the low-density region of the liquid/vapor interface of water modeled with the Lemberg–Stillinger–Rahman (LSR) potential. They interpreted this molecular relaxation only in light of a reduction in the average number of interfacial hydrogen bonds per molecule, but it is probable that this result also provides qualitative evidence for an expansion of the O–O distance that naturally accompanies a contraction of the covalent OH distance. The covalent OH bond length is anticorrelated with intermolecu-

lar O–O distance, which is a well-documented trend exhibited in a variety of hydrogen bonding systems. Such results have been compiled into a ''universal'' curve as described in Ref. 32. Consequently, a 0.5% contraction of the covalent distance observed by Townsend and Rice implies an approximate expansion of the intermolecular O–O distance of 4%, strikingly consistent with the expansion determined experimentally in this study. However, this estimate of the OH distance is also a sensitive to the O–HO angle, which is not specifically accounted for in these compilations. In addition, it is unclear whether this intramolecular relaxation observed at the water interface is a general phenomenon reproduced by competing water force fields or merely an artifact of the LSR potential.

In contrast to water, the surface vibrational spectrum of liquid methanol shows no evidence of a ''free OH'' bond.[9] The ''bonded OH stretching'' region exhibits a vibrational band that is much narrower than and redshifted from the bulk liquid infrared spectrum. The close correspondence of the SFG spectrum to that measured for solid methanol led Stanners *et al.*[9] to conclude that the surface of liquid methanol is ''icelike.'' The O–O distance in solid methanol has been previously determined by diffraction methods to be 2.66 Å,[33] implying a shorter hydrogen bond length than in the liquid, which is consistent with the observed redshifted vibrational spectrum. The surface R_{O-O} for liquid methanol measured by TIY EXAFS is 2.62 ± 0.05 Å, which is in close agreement with the result described above. Solid methanol contains molecules arranged in parallel hydrogen bonded chains with an average of two hydrogen bonds per molecule. The close correspondence of the O–O distance and vibrational spectrum of the liquid surface with that of solid methanol leads to the conclusion that a similar hydrogen bond topology is present at the liquid surface. The strong orientation of the methyl group in the outermost surface layer naturally implies an oppositely oriented adjacent layer below the surface. This ''hydrophobic packing'' minimizes steric effects, allowing a stronger and thus shorter hydrogen bond between interfacial methanol molecules. Such polar ordering at the interface might induce or nucleate the formation of chains, analogous to solid methanol, which would quickly branch into the less-ordered hydrogen bonded structure characteristic of the bulk liquid. In a recent paper by Yeh *et al.*,[34] the acetone liquid/vapor interface was also observed to show polar ordering similar to methanol and characteristic of a solid acetone phase.

Theoretical studies of hydrogen-bonded clusters have shown that the binding energy of the methanol dimer (6.04 kcal/mol) is larger than that of the water dimer (5.13 kcal/mol),[35] given the same level of calculation. Matsumoto *et al.*[36] observed methanol dimers evaporating directly from the liquid surface in the course of studying evaporation dynamics with MD simulations. No such findings were reported for liquid water in their subsequent studies of aqueous evaporation. In the course of our own studies we have observed methanol dimers in the gas phase above the liquid surface by detecting products of core-level excitation, whereas no such clusters have been observed from liquid water microjets under the same experimental conditions. While this result is preliminary, it seems to support the notion that the interfacial hydrogen bond between neighboring methanol molecules is indeed stronger than in water and that a significant number of these bonds do remain intact during evaporation. Furthermore, this corroborates the present evidence for stronger hydrogen bonds at the surface of liquid methanol provided by the observation of a shorter O–O interfacial distance.

The contraction of the surface O–O distance in methanol and the corresponding expansion in water appear counterintuitive when one examines the surface tension of these liquids. In the absence of interfacial ordering, the shorter O–O distance would seem to imply a larger surface tension for liquid methanol than for water. However, the strong orientation of the methyl group about surface normal implies that the lateral interactions between molecules at the interface are weaker, dominated by dispersion forces between methyl groups. This is the case in liquid hexane and would explain the close correspondence between the surface tension of hydrocarbons and their alcohol analogs. Water, on the other hand, can form a larger number of interfacial bonds in a variety of configurations (acceptor only, single donor, double donor, etc.) with networks extending perpendicular as well as parallel to the interface.

Finally, it has also been pointed out by Luck[37] that when one compares the surface free energy of water with that of other solvents (e.g., methanol, ethanol, acetone, etc.) on a per molecule basis, the differences among these liquids are much less pronounced. For example, the surface free energy of methanol is 3.53×10^{-21} J/molecule (assuming 16 Å^2 per molecule), while the corresponding value in water is only a factor of 2 larger (7.0×10^{-21} J/molecule). This implies that the abnormally large surface tension in water is due in part to the larger number density at the water interface. The remaining difference between the water and methanol surface probably reflects the reduced number of interfacial hydrogen bonds per methanol molecule. However, care must be taken in reporting the average free energy per molecule, as one must assume a cross-sectional area which can be difficult to estimate for polar oriented asymmetric molecules.

The expansion of the O–O distance at the liquid water surface and the corresponding contraction in liquid methanol provide new insights into the decomposition of the bulk hydrogen bond structure at these interfaces. Methanol and water, two of the simplest hydrogen-bonded liquids, exhibit dramatically different hydrogen bond topologies, which become more pronounced at the interface. Methanol molecules tend to form planar or chain structures in the bulk liquid which is enhanced at the surface by polar ordering, yielding an O–O distance and SFG spectrum similar to solid methanol. On the other hand, the expansion of the O–O distance in water is consistent with the relaxation of the covalent OH distance and dipole moment observed in molecular dynamics simulations, suggesting an interfacial phase of more mobile water molecules. The structural details reported here can be directly compared to the RDF's computed in MD simulations, thus providing benchmarks for the development of more realistic liquid models. Furthermore, to accurately account for intermolecular surface relaxation, it would appear necessary

to employ flexible and polarizable liquid force fields. X-ray spectroscopy of liquid microjets should provide a novel way to examine the electronic and geometric structure of volatile liquid interfaces which are presently inaccessible via other experimental techniques.

ACKNOWLEDGMENTS

This work is supported by the Experimental Physical Chemistry Program of the National Science Foundation. K.R.W. is supported by a Doctoral Fellowship in Residence at the Advanced Light Source, Lawrence Berkeley National Laboratory. The authors also acknowledge the outstanding technical support provided by John Pepper (ALS), Eric Granlund (UCB), and the UCB chemistry machine shop.

[1] G. A. Somorjai, *Introduction to Surface Chemistry and Catalysis* (Wiley, New York, 1994).
[2] A. K. Soper, F. Bruni, and M. A. Ricci, J. Chem. Phys. **106**, 247 (1997).
[3] A. H. Narten and H. A. Levy, J. Chem. Phys. **55**, 2263 (1971).
[4] A. Adya, L. Bianchi, and C. Wormald, J. Chem. Phys. **112**, 4231 (2000).
[5] T. Takamuku, T. Yamaguchi, M. Asato, M. Matsumoto, and N. Nishi, Z. Naturforsch., A: Phys. Sci. **55**, 513 (2000).
[6] G. Hura, J. Sorenson, R. M. Glasser, and T. Head-Gordon, J. Chem. Phys. **113**, 9140 (2000).
[7] D. L. Wertz and R. K. Kruh, J. Chem. Phys. **47**, 388 (1967).
[8] Q. Du, R. Superfine, E. Freyz, and Y. R. Shen, Phys. Rev. Lett. **70**, 2313 (1993).
[9] C. D. Stanners, Q. Du, R. Chin, P. Cremer, G. A. Somerjai, and Y. R. Shen, Chem. Phys. Lett. **232**, 407 (1995).
[10] K. Wolfrum, H. Graener, and A. Laubereau, Chem. Phys. Lett. **213**, 41 (1993).
[11] R. M. Townsend and S. A. Rice, J. Chem. Phys. **94**, 2207 (1991).
[12] R. S. Taylor, L. X. Dang, and B. C. Garrett, J. Phys. Chem. **100**, 11720 (1996).
[13] L. X. Dang and T. S. Chang, J. Chem. Phys. **106**, 8149 (1997).
[14] M. Matsumoto and Y. Kataoka, J. Chem. Phys. **88**, 3233 (1988).
[15] J. Alejandre, G. Chapela, and D. Tildesley, J. Chem. Phys. **102**, 4574 (1995).
[16] M. Matsumoto and Y. Kataoka, J. Chem. Phys. **90**, 2398 (1989); **95**, 7782(E) (1991).
[17] Kevin R. Wilson, B. S. Rude, T. Catalano, R. D. Schaller, J. G. Tobin, D. T. Co, and R. J. Saykally, J. Phys. Chem. B **105**, 3346 (2001).
[18] Kevin R. Wilson, M. Cavalleri, B. S. Rude, R. D. Schaller, A. Nilsson, L. G. M. Pettersson, N. Goldman, T. Catalano, J. D. Bozek, and R. J. Saykally, J. Phys.: Condens. Matter **14**, L221 (2002).
[19] E. A. Stern, Phys. Rev. B **10**, 3027 (1974).
[20] A. Bianconli, Appl. Surf. Sci. **6**, 392 (1980).
[21] B. K. Teo, *EXAFS: Basic Principles and Data Analysis*, Inorganic Chemistry Concepts, Vol. 9 (Springer, Berlin, 1986).
[22] Kevin R. Wilson, J. G. Tobin, A. L. Ankudinov, J. J. Rehr, and R. J. Saykally, Phys. Rev. Lett. **85**, 4289 (2000).
[23] B. X. Yang and J. Kirz, Phys. Rev. B **36**, 1361 (1987).
[24] B. K. Teo and P. A. Lee, J. Am. Chem. Soc. **101**, 2815 (1979).
[25] D. T. Bowron, M. H. Krisch, A. C. Barnes, J. L. Finney, A. Kaprolat, and M. Lorenzen, Phys. Rev. B **62**, R9223 (2000).
[26] K. L. Klementev, Nucl. Instrum. Methods Phys. Res. A **448**, 299 (2000).
[27] T. Weitkamp, J. Neuefeind, H. E. Fischer, and M. D. Zeidler, Mol. Phys. **98**, 125 (2000).
[28] A. Filipponi, J. Phys.: Condens. Matter **13**, R23 (2001).
[29] A. Filipponi, J. Phys.: Condens. Matter **6**, 8415 (1994).
[30] F. N. Keutsch and R. J. Saykally, PNASL **98**, 10 533 (2001).
[31] J. B. Paul, C. P. Collier, R. J. Saykally, J. J. Scherer, and A. O'Keefe, J. Phys. Chem. **101**, 5211 (1997).
[32] P. Schuster, G. Zundel, and C. Sandorfy, *The Hydrogen Bond* (North-Holland, Amsterdam, 1976), Vol. II, p. 411.
[33] K. J. Tauer and W. N. Lipscomb, Acta Crystallogr. **5**, 606 (1952).
[34] Y. Yeh, C. Zhang, H. Held, A. M. Mebel, X. Wei, S. H. Lin, and Y. R. Shen, J. Chem. Phys. **114**, 1837 (2001).
[35] R. A. Provencal, K. Roth, J. B. Paul, C. N. Chapo, R. N. Casaes, R. J. Saykally, G. S. Tschemper, and H. F. Schaefer, J. Phys. Chem. A **104**, 1423 (2000).
[36] M. Matsumoto, K. Yasuoka, and Y. Kataoka, J. Chem. Phys. **101**, 7912 (1994).
[37] W. A. P. Luck, Colloid Polym. Sci. **279**, 554 (2001).